Characteristics of Suspended Sediment Transport in the Surf Zone of Irregular Waves and their Reproduction by a Cross-Shore Beach Deformation Model

M. Ikeno[1] and T. Shimizu[1]

Abstract

Suspended sediment flux and cross-shore beach deformation in the breaker zone are elucidated experimentally with the CRIEPI's irregular wave flumes of large and middle sizes. Effects of long waves on suspended sediment transport are also investigated with a new experimental system for correct reproduction of infragravity waves bounded by irregular wave groups. Based on the experimental results, the pick up rate from sea bed and convection and diffusion of suspended sediment are modelled, and a new numerical model is developed for cross-shore beach deformation due to irregular waves. This numerical model can well reproduce wave deformation, suspended concentration, undertow, sediment flux and beach topography change.

1. INTRODUCTION

In the surf zone, sea bed sands are picked up violently and suspended sediment transports are more signifficant. A numerical model for beach deformation due to ramdom waves should be developed by taking irregular time variation of suspended sediment flux into account..

In this paper, first, suspended sediment flux and cross-shore beach deformation in the breaker zone are elucidated experimentally with the CRIEPI's irregular wave flumes of large and middle sizes. Scale effects on beach deformation are also investigated, and a new similarity law of the grain size of beach sediment is applied to irregular waves. Effects of long wave components on suspended sediment transport are also investigated with a new experimental system for correct reproduction of infragravity waves bounded by irregular wave groups.

Secondly, based on the experimental results, the pick up rate from the sea bed and vertical convection and diffusion of suspended sediment are modelled, and a new numerical model is developed for cross-shore beach deformation due to irregular waves. Nonlinear wave deformation, suspended concentration, undertow, sediment flux, and beach topography change in experiments are reproduced by this numerical model.

2. EXPERIMENT

2.1 Experimental condition

Beach deformation tests were performed with two different scales of wave flumes

---

[1] Hydraulics Dept., Central Res. Inst. of Electric Power Industry, 1646 Abiko, Abiko-shi, Chiba, Japan

and compared. One is a large wave flume (205m long, 3.4m wide and 6m deep). The median grain size of sand used is 1mm. Initial beach slopes are changed from 1/10 to 1/50. Incident waves are irregular with JONSWAP spectrum. Significant wave heights and periods are $0.5 \sim 1.2$m and $3 \sim 8$s. Sharpness parameter γ are 1 or 7 (experimental cases L1~L7; Shimizu and Ikeno, 1996). The other is a middle wave flume (50m long, 0.9m wide and 1.2m deep). The scale of beach deformation tests corresponds to one-fifth the scale of those with the above large wave flume by the Froude similitude. Initial beach slope, significant wave height, period and parameter γ are similar values to those with the above large wave flume. Significant wave heights and periods are $0.1 \sim 0.24$m and $1.35 \sim 3.58$s (experimental cases M1~M8).

However, using the sand size according to the Froude similitude, the scale effects on beach deformation will occur between the middle and large sizes of tests, as you know. In this paper, the sand size is determined by a new similarity law of the grain size of beach sediment (see Fig.1 ; Shimizu, 1995), based on many different scales of beach deformation tests in regular waves. According to Fig.1, the median grain size of sand is determined to 0.6 mm, which corresponds to one half the scale of sand in the above large wave flume. Comparing both experimental results, the validity of this similarity law is verified subject to irregular waves.

Fig.2 shows the grain size distribution of sands used in the large and middle scale tests. In these experiments, vertical distribution of suspended sediment transport flux in the surf zone are measured simultaneously by optical turbidimeters, electromagnetic current meters and capacitance type wave gauges.

2.2 Verification of a new similarity law of sand grain size

Fig.3 shows the comparison between beach deformation results by large and middle wave flumes. Beach deformation of these cases is erosion type by plunging breaking waves. One is the case L6: H_s=1.2m, T_s=3s, $\tan \beta$ =1/10, and the other is the case M7: H_s=0.24m, T_s=1.35s, $\tan \beta$ =1/10. The formation points of bar and the erosional regions in the large scale test show good agreement with those of the middle
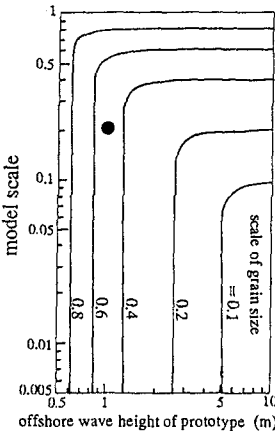
Fig.1 Model scale and grain size considering the scale effect (Shimizu, 1995)
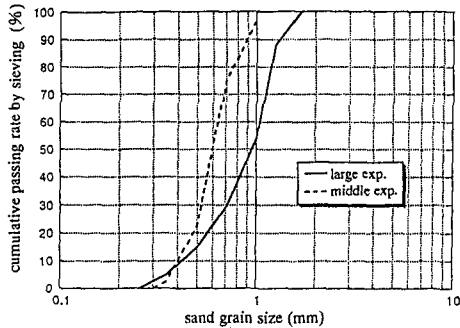
Fig.2 Grain size distribution of sands used in the large and middle size tests

case L6: H_o=1.2m, T_o=3s, γ =7, tan β =1/10, BLOWRES
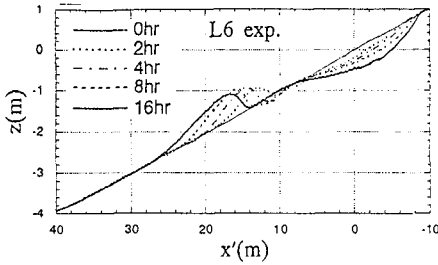
case M7: H_o=0.24m, T_o=1.35s, γ =7, tan β =1/10, BLOWRES
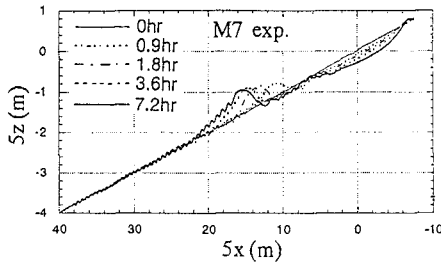
Fig.3 Comparison between beach deformation results by large and middle wave flumes
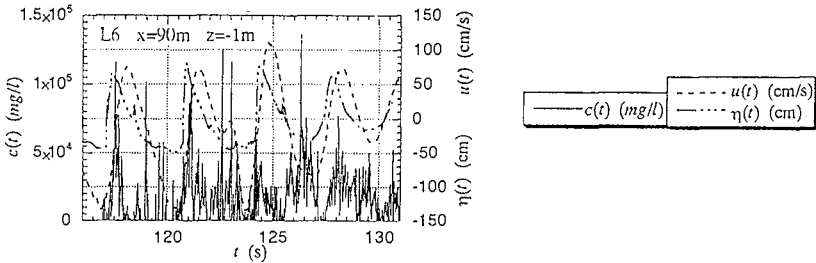
Fig.4 Time variation of suspended concentration and horizontal velocity in the surf zone of irregular waves (case L6 of large scale test)
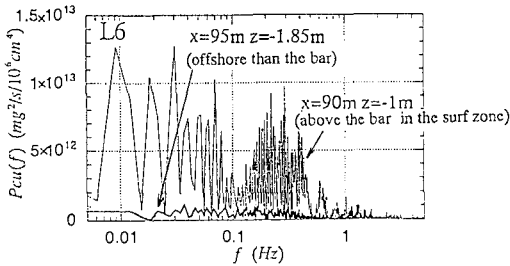
Fig.5 Power spectra of the suspended sediment flux $c(t)u(t)$ at the vertical height 20cm above the sea bottom in the case L6 of large scale tests

test. And the velocity of beach changes in the large test also shows good agreement with that according to the Froude similitude in the middle test. And thus, the application of this new similarity law of the grain size (Shimizu, 1995) to random waves is verified.

2.3 Effects of long waves on suspended sediment

Fig.4 shows time variation of suspended concentration and horizontal velocity near the sea bottom and water surface elevation in the surf zone of irregular waves. According to Fig.4, the sea bed sand can be seen to be significantly picked up when the horizontal velocity changes not only from onshore to offshore, but also from offshore to onshore.

Effects of long waves on suspended sediment flux are also investigated with a new experimental system, which can correctly reproduce bounded long waves in irregular wave groups by eliminating free long waves generated by a wave maker (BLOWRES ; Ikeno and Tanaka, 1996).

Fig.5 shows the power spectra of the suspended sediment flux c(t)u(t) at the vertical height 20cm above the sea bottom in the case L6 of large scale tests. In this figure, a fine solid line corresponds to the formation point of bar in the surf zone, and a bold solid line corresponds to the offshore side than it. From Fig.5, the suspended sediment flux can be seen to be separated into the the higher and the lower frequency components as the boundary of 0.07Hz. Especially, the long wave components of the suspended flux above the bar in the surf zone are much greater than the short components of it. According to these experimental results, three kinds of components such as the steady: $\dot{c}\dot{u}$, the shorter waves: $\overline{cu}_s$, the longer waves: $\overline{cu}_l$ as the boundaries of 0.16Hz: middle tests and 0.07Hz: large tests, are included in the suspended sediment flux due to random waves. So, each component of the suspended flux is evaluated as the time-averaged (net) values of c(t)u(t) obtained by the inverse FFT after cutting the flux except the remarkable frequency region.

Fig.6 shows the vertical distribution of three kinds of the flux components in the middle scale tests. This corresponds to th-

case M5: H_o=0.2m, T_o=2.2s, γ=1, tan β=1/20, BLOWRES
case M2: H_o=0.2m, T_o=2.2s, γ=1, tan β=1/20, ordinary
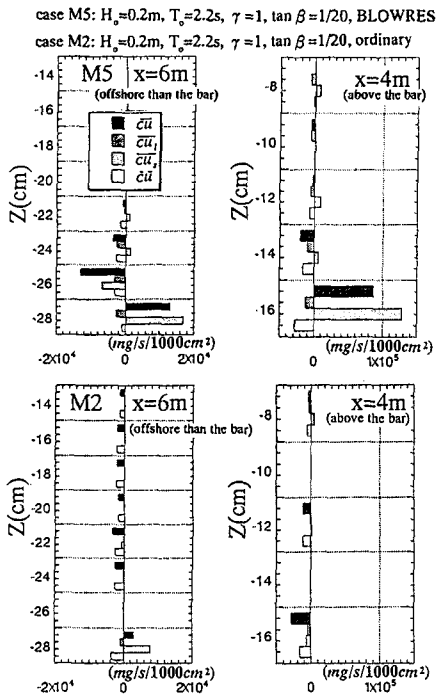
Fig.6 Vertical distribution of three kinds of the flux components in the middle scale tests
(tan β=1/20, spilling wave breaking and wider surf zone)

e case of the sea bed slope 1/20, the spilling wave breaking and the wider surf zone. In this figure, the upper figures are the results with the new experimental system for correct reproduction of infragravity waves; BLOWRES. And the lower figures are those without using it; ordinary.

Comparing between the upper and the lower figures, specially, the difference can be seen between the direction and the quantities of long wave components of the suspended sediment flux in the tests with and wthout eliminating free long waves. This difference becomes more significant in the case of the wider surf zone.

The long period and steady components of suspended sediment flux in the surf zone are generally offshore direction while the short period components of suspended sediment flux are onshore direction. Its steady components increase more than the short and long period components with shoaling and breaking.

3. NUMERICAL MODEL

A numerical model is developed for cross-shore beach deformation due to nonlinear irregular waves. This numerical model consists of the following sub-models.

3.1 Irregular wave deformation

The improved Boussinesq equation (Madsen et al.,1991) with a breaker-induced energy dissipation term (Sato and Kabiling,1994) is adopted as follows:

$$\frac{\partial \eta}{\partial t} + \frac{\partial Q}{\partial x} = 0 \tag{1a}$$

$$\begin{aligned}
\frac{\partial Q}{\partial t} &+ \frac{\partial}{\partial x}\left(\frac{Q^2}{D}\right) + gD\frac{\partial \eta}{\partial x} \\
&= \left(B + \frac{1}{3}\right)h^2\frac{\partial}{\partial t}\left(\frac{\partial^2 Q}{\partial x^2}\right) + Bgh^3\frac{\partial^3 \eta}{\partial x^3} + \nu_e\frac{\partial^2 Q}{\partial x^2}
\end{aligned} \tag{1b}$$

where η is the water surface elevation, Q is the depth-integrated flow rate in the horizontal ditrection, h is the still water depth, D is the total water depth (=h+ η), g is the acceleration due to gravity, B is a parameter for improving linear dispersion and equal to be 1/21 (Madsen et al.,1991), ν_e is the eddy viscosity for momentum mixing exchange due to turbulence by wave breaking (Sato and Kabiling,1994).

3.2 Vertical distribution of velocity in the surf zone of irregular waves

Relationship between the horizontal velocity u at the arbitrary vertical position z and vertically averaged velocity $\ddot{u}$ is derived by Nwogu (1993) as follows:

$$u(z,t) = \ddot{u}(t) + \left\{\frac{h^2}{6} - \frac{(h+z)^2}{2}\right\}\frac{\partial^2 \ddot{u}(t)}{\partial x^2} \tag{2a}$$

where $\ddot{u}(t) = Q(t)/(h+\eta)$, z is the vertical position positive above the still water level.

In the above Eq.(2a) based on the Boussines type equation , undertow caused by wave breaking can't be taken into account. So, the vertical distribution of undertow must be added to the above Eq.(2a) by using the another method. In this paper, the vertical distribution of undertow is added as time-averaged velocity based on the eddy viscosity model. The regular wave undertow formula (Rattanapitikon and

Shibayama,1996) proposed by Okayasu et al. (1990) is modified to apply to irregular wave undertow obtained by the large and middle scale of cross-shore beach deformation tests.

As results, the vertical distribution $\ddot{u}(z)$ of undertow of irregular waves is proposed by taking into account the energy dissipation D_B due to wave breaking on the basis of the bore model (Thornton and Guza, 1983) as follows:

$$D_B = \rho g H_s^3 / 4 T_s h \qquad (2b)$$

$$\ddot{u}(z) = \rho^{1/3} D_B^{1/3} \left[(z+h)/h - 0.5 - 0.22 \cdot \ell n \left\{ (z+h)/h \right\} \right] - 0.1 \frac{\sqrt{gh} H_s}{h} \qquad (2c)$$

where H_s is the significant wave height, ρ is fluid density, T_s is the significant wave period.

3.3 Suspended sediment concentration

The time variation of sediment concentration due to combined convection-diffusion is calculated by using the following equation :

$$\frac{\partial c}{\partial t} = w_s \frac{\partial c}{\partial z} + \varepsilon_s \frac{\partial^2 c}{\partial z^2} + \frac{1}{w_c} \exp\left(-\frac{z+h}{L_s}\right) \dot{p}\left(t - \frac{z+h}{w_c}\right) + \frac{1}{L_s} p\left(t - \frac{z+h}{w_c}\right) \exp\left(-\frac{z+h}{L_s}\right) \quad (3a)$$

where, c is the sediment concentration, p is the pick up rate from sea bed, w_s is the settling velocity (sand grain size 1mm; 0.095m/s).

L_s is the scale of suspended sediment distribution (Nielsen ,1992) as follows:

$$L_s = \begin{cases} 0.15\pi a f/w_s & \text{for } 2\pi a f/w_s \leq 18 \\ 1.4\zeta & \text{for } 2\pi a f/w_s \geq 18 \end{cases} \qquad (3b)$$

where ζ is the sand ripple height (0.15m from large experiments), f is the significant wave frequency, a is the significant wave amplitude.

ε_s is the sediment diffusivity (Nielsen,1988) as follows:

$$\varepsilon_s = w_s \zeta \left[1.24 \exp\left\{ -40 \left(\frac{\ddot{u}}{u_b} \right)^2 \right\} + 0.2 \right] \qquad (3c)$$

where $\hat{u}$ is the amplitude in a half period by zero-crossing the horizontal velocity nearthe sea bottom.

w_c is the vertical convection velocity of sediment by Sleath (1987) as follows:

$$w_c \approx 2\pi f \delta_{05} / 2.27 \qquad (3d)$$

where δ_{05} is the thickness of boundary layer as follows:

$$\delta_{05} = 0.26 r (a/r)^{0.7} \qquad (3e)$$

where r is the roughness (=d), d is the sand grain size.

w_c, ε_s and L_s are time-varying, corresponding to the zero-crossing amplitude of velocity u near the sea bottom.

Boundary condition at the sea bottom is as follows:
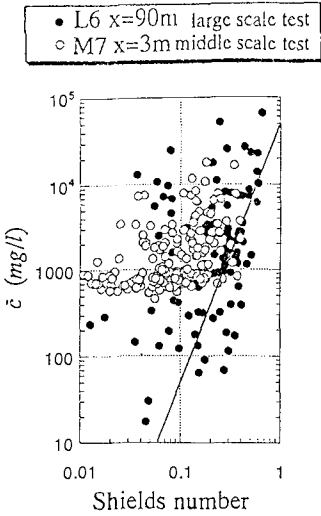
Fig.7 Relationship between the time-averaged
suspended concentration in a half period
by zero-crossing the horizontal velocity
near the sea bottom and the Shields number
corresponding to a half period just before it
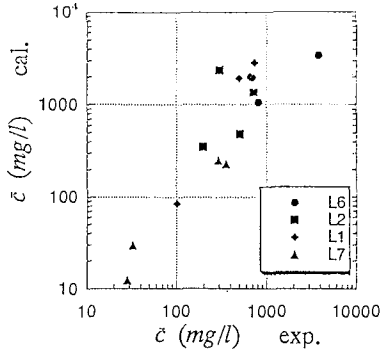
Fig.8 Comparison between the time-averaged suspended
concentration computed and measured at the height
of 20cm above the sea bottom in the large scale cases
of L1~L7

$$-\varepsilon_s \frac{\partial c}{\partial z} = 0 \qquad at\ z = -h \qquad (3f)$$

Fig.7 shows the relationship between the time-averaged suspended concentration in a half period by zero-crossing the horizontal velocity near the sea bottom and the Shields number corresponding to a half period just before it. These data are measured near the sea bottm formating the bar in the surf zone, where the concentration is the highest in the large and middle scale tests. According to Fig.7, high correlation can be seen between the suspended concentration and the Shields number just before it. Especially, heigher concentration in the large scale tests, which means the pick up rate is much, can be also seen to be proportional to the 1.5th power of the Shields number just before it.

Based on the above experimental results, the pick up rate p(t) is newly modelled as follows:

$$p(t) = \alpha_s w_s \rho_s (\psi_{i-1} - \psi_c)^{1.5} \delta(t - t_i) \qquad (3g)$$

where ρ_s is sediment density $(=2.65), \delta(t-t_i)$ is the delta function, and t_i is the zero-crossing time of velocity u near the sea bottom.
α_s is a parameter proposed based on experimental results as follows:

$$\alpha_s' = \begin{cases} \left(H_0/L_0\right)\left(-\lambda + 2.3\right) & for\ \lambda \geq 1.3 \\ \left(H_0/L_0\right)\left(0.62\lambda + 0.2\right) & for\ \lambda \leq 1.3 \end{cases} \qquad (3h)$$

$$\alpha_s = \max\left\{\alpha_s' , 0.01\right\} \tag{3i}$$

where $\lambda = h/(H_0 \log^{(1/\tan\beta)})$, H_0 and L_0 are the offshore significant wave height and the wave length, $\tan \beta$ is the sea bed slope. ψ_c is the critical Shields number, ψ_{i-1} means the Shields number of the 'i-1' th zero-crossing wave in a half period. Eq.(3h) and (3i) are based on the experimental results in the cases of $H_0/L_0 \geqq 0.02$.

Fig.8 shows the comparison between the time-averaged suspended concentration computed and measured at the height of 20cm above the sea bottom in the large scale cases of $L1 \sim L7$. The computed values show good agreements with the experimental values.

3.4 Sediment transport rate and sediment conservation equation

The suspended sediment transport rate is estimated by integrating the sediment flux **cu** in the vertical section as follows:

$$q_s(t) = \int_{-h}^{0} c(z,t)\, u(z,t) dz \tag{4a}$$

The bed load transport rate is estimated by the following formula proposed by Sato and Kabiling (1994).

$$q_b(t) = \sqrt{\left(\frac{\rho_s}{\rho_w} - 1\right) g d^3}\, \alpha_b \left|\psi(t)\right|^{0.5} \max\left\{\psi(t) - \psi_c, 0\right\} u_b(t) \Big/ \left|u_b(t)\right| \tag{4b}$$

where α_b is a parameter ($=1$), ψ_c is the critical Shields number.

Therefore, the total sediment transport rate is as follows:

$$q(t) = q_s(t) + q_b(t) \tag{4c}$$

Finally, the sea bed topography is updated by using the following sediment conservation equation.

$$\frac{\partial z_b}{\partial t} = -\frac{\partial h}{\partial t} = -\frac{\partial}{\partial x}\left\{\tilde{q} - \varepsilon_b \left|\tilde{q}\right| \frac{\partial z_b}{\partial x}\right\} \tag{4d}$$

where z_b is the vertical height of sea bed, $\tilde{q}$ is the time-averaged (net) total sediment transport rate, ε_b is a coefficient that reflects the effect of local bottom slope on the sediment transport ($=2.0$).

During the offshore rush in the swash zone, the total water depth is less than that during the onshore rush so larger velocities will result during the offshore rush. In order to avoid unrealistic erosion, the net total sediment transport rate in the swash zone is linearly interpolated between the zero sediment transport corresponding to the maximum beach run-up height, and the sediment transport at the most onshore side position computing the suspended sediment and bed load rates actually, where the still water depth is equal to $\triangle z$ divided vertically in combined convection-diffusion computation of suspended concentration (Larson, 1994).

START

input of initial sea bed topography
offshore sign. wave height, period
random wave computation time t_w
sea bed update time t_b
wave action time t_{total}

random wave deformation comp.
(Improved Boussinesq Eq.)

vertical distribution of
undertow by breaking
(eddy viscosity model)

comp. of time variation of water surface
elevation and vertically averaged velocity

time variation of velocity at the arbitrary z

time variation of velocity near sea bottom

comp. of pick up rate

combined convection-diffusion comp.

time variation of concentration at the arbitrary z

time variation of suspended sediment flux at z

time variation of bed load
transport

time variation of suspended sediment
transport

time variation of total load
transport

averaging by t_w

comp. of sea bed change
(conservation eq.)

$t < t_b$

YES   NO

update of sea bed

$t < t_{total}$

YES   NO

STOP

Fig.9 Computation flow of this new cross-shore beach deformation model

Fig.9 explains the computation flow of this new cross-shore beach deformation model. In this numerical model, first, the irregularly varying physical quantities such as the wave deformation, the suspended concentration, the coss-shore bed load and suspended sediment transport rates, are computed in the interval of the random wave computation time t_w, corresponding to one hundred waves' time. If required, the vertical distribution of undertow by wave breaking is added as the time-averaged values to the time variation of the horizontal velocity at the arbitrary position z obtained by the improved Boussinesq equation. Next, the net total sediment rate averaged by t_w is computed, and input on the sediment conservation equation. This sediment conservation equation continues to be computed until the sea bed update time t_b. After passing t_b, the sea bed topography is updated. After that, using a new sea bed topography, the above physical quantities are computed in the same interval of t_w and repeated.

4. REPRODUCTION BY THIS NUMERICAL MODEL

4.1 Reproduction of the vertical distribution of suspended concentration, flux and velocity in the surf zone of irregular waves

Figs.10 and 11 show the comparison between the vertical distribution of time-averaged velocity in the surf zone by computation and experiments. In the computation, the vertical distribution of irregular wave undertow is added to that of velocity by the improved Boussinesq equation. Fig.10 corresponds to the large size tests, and Fig.11 corresponds to the middle size tests. According to these figures, computation results with the undertow formula can well reproduce the vertical distribution of time-averaged velocity in the surf zone of irregular waves.

Figs.12 and 13 show the comparison between the time variation and the vertical distribution of suspended concentration in the surf zone of irregular waves by computation and experiments. In Figs.12 and 13, computation results include those by pure diffusion without convection and by combined convection-diffusion. According to these figures, suspended concentration by the pure diffusion computation can't reach into the upper area near the water surface and underestimates the experimental suspended concentration. However, the computation results by combined convection-diffusion can well reproduce the irregular time variation and the vertical distribution of experimental results, where suspended sediment with higher concentration reaches near the water surface. Fig.14 shows the comparison between the vertical distribution of time-averaged suspended sediment flux by computation with combined convection-diffusion and experiments. According to Fig.14, the computation results can well reproduce the vertical distribution of time-averaged suspended sediment flux.
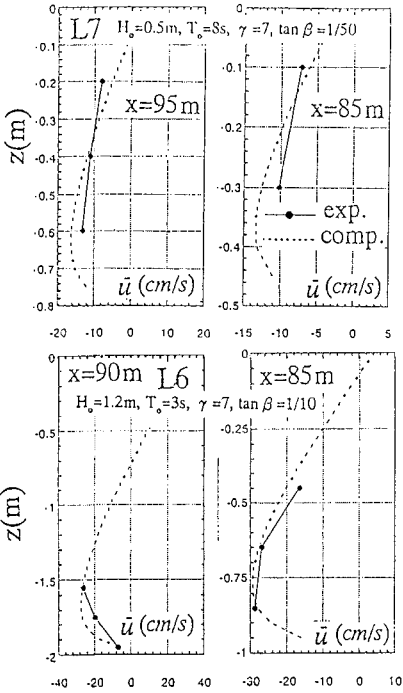
Fig.10 Comparison between the vertical distribution
of time-averaged velocity in the surf zone by
computation and large scale tests

exp.
comp. pure diffusion
comp. combined convection-diffusion
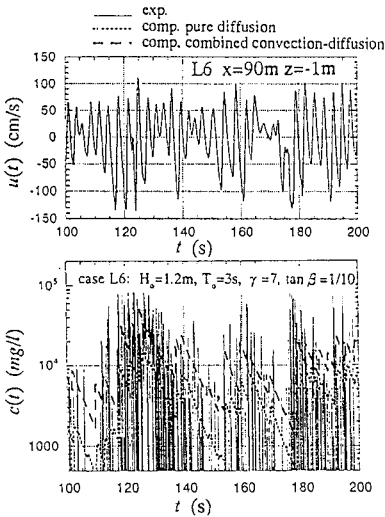
Fig.12 Comparison between the time variation of suspended
concentration in the surf zone of irregular waves by
computation and experiments

4.2 Reproduction of wave deformation, beach change and sediment transport rate

Figs.15 and 16 show the comparison between sea bed changes, wave height deformation and sediment transport rates by computation and large size experiments. Computation results include the cases

$H_o=0.24m$, $T_o=1.35s$, $\gamma =7$, $\tan \beta =1/10$
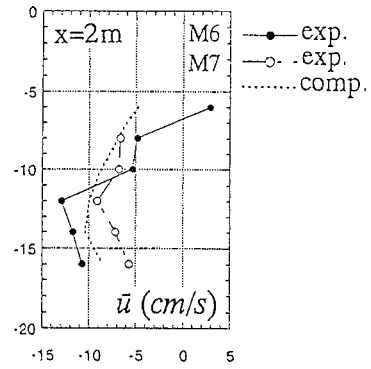
Fig.11 Comparison between the vertical
distribution of time-averaged velocity
in the surf zone by computation and
middle scale tests

comp. combined convection-diffusion
comp. pure diffusion
exp.
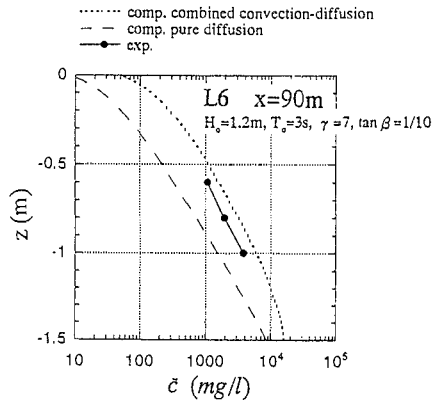
Fig.13 Comparison between the vertical distribution of time-
averaged suspended concentration by computation
and experiments

$H_o=1.2m$, $T_o=3s$, $\gamma=7$, $\tan\beta=1/10$ $\qquad$ $H_o=0.5m$, $T_o=8s$, $\gamma=7$, $\tan\beta=1/50$
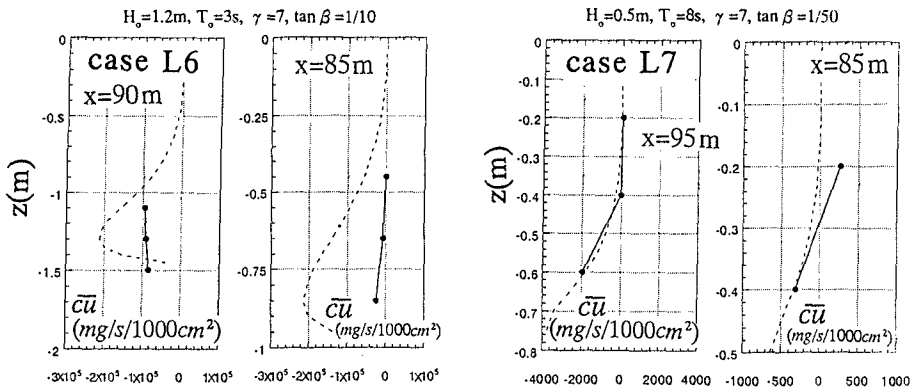
Fig.14 Comparison between the vertical distribution of time-averaged suspended sediment flux by computation with combined convection-diffusion and experiments
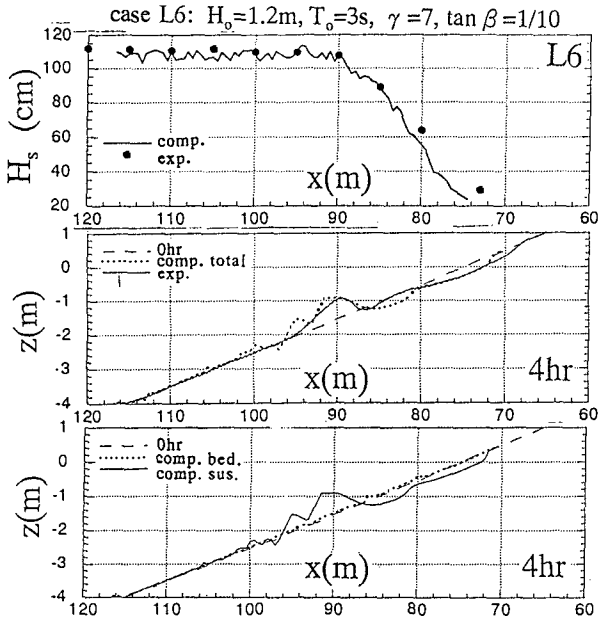
Fig.15 Comparison between irregular wave deformation and sea bed changes by computation and large size experiments

taking into account the suspended sediment alone, the bed load alone and the total sediment transport. According to thesefigures, the computation results can well reproduce the experimental sea bed changes, wave height deformation and total sediment transport rate. The suspended sediment transport rate is much greater than the bed load transport rate in the case L6 with larger wave height.

H_o=1.2m, T_o=3s, γ =7, tan β =1/10
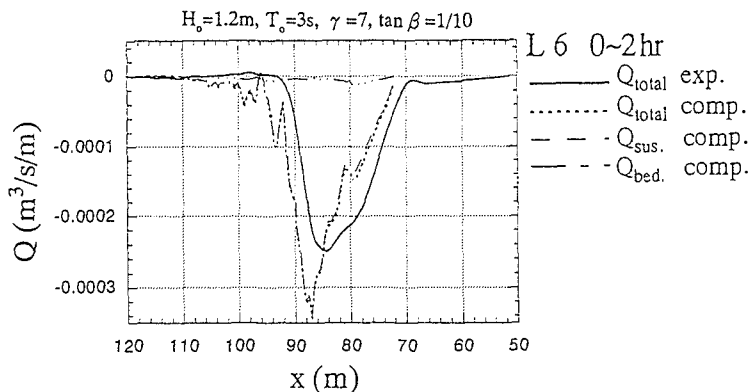
Fig.16 Comparison between sediment transport rates
by computation and large size experiment

CONCLUSIONS AND REMARKS

1) Beach deformation and suspended sediment flux in the large scale tests showed good agreement with those in the middle scale tests. And thus, the application of this new similarity law of sand grain size (Shimizu, 1995) to random waves is verified.

2) In all cases, the difference can be seen between long period components of suspended sediment flux in the tests with and without eliminating free long waves. This difference becomes more significant in the case of the wider surf zone.

3) The long period and steady components of suspended sediment flux in the surf zone are generally offshore direction while the short period components of suspended sediment flux are onshore direction. Its steady components increase more than the short and long period components with shoaling and breaking.

4) This numerical model can well reproduce irregular time variation such as nonlinear wave deformation, suspended concentration, velocity and sediment flux and beach topography change.

5) Suspended load is much greater than bed load in the case of large wave height.

REFERENCES

Ikeno, M. and H.Tanaka (1996) : A New Experimental System for Reproduction of Infragravity Waves Bounded by Irregular Wave Groups and their Wave Deformation, CRIEPI Abiko Res. Lab. Rep. No.U95042 (in Japanese).

Ikeno, M. and T. Shimizu (1997) : Characteristics of Suspended Sediment Transport in the Surf Zone of Irregular Waves and their Reproduction by a Cross-Shore Beach Deformation Model, CRIEPI Abiko Res. Lab. Rep. No.U96037 (in Japanese).

Larson, M. (1994) : Predictive Beach Profile Change at Mesoscale under Random

Waves, Proc. 24th Int. Conf. on Coastal Eng., pp.2252-2266.

Madsen, P. A., R. Murrary and O. R. Sorensen (1991) : A new form of the Boussinesq equations with improved linear dispersion characteristics, Coastal Eng., Vol.15, pp.371-388.

Nielsen, P. (1984) : Field measurements of time-averaged suspended sediment concentrations under waves, Coastal Eng., Vol.8, pp.51-72.

Nielsen, P. (1988) : Three simple models of wave sediment transport, Coastal Eng., Vol.12,pp.43-62.

Nielsen, P. (1992) : Coastal Bottom Boundary Layers and Sediment Transport, Advanced Series on Ocean Engineering, Vol.4, World Scientific, pp.201-262.

Nwogu, O. (1993) : Alternative Form of Boussinesq Equations for Nearshore Wave Propagation, J. of Waterway, Port, Coastal, and Ocean Engineering, Vol.119, No.6, ASCE, pp.618-628.

Okayasu, A., A.Watanabe and M.Isobe (1990) : Modeling of Energy Transfer and Undertow in the Surf Zone, Proc. 22th Int. Conf. on Coastal Eng., ASCE, pp.123-135.

Rattanapitikon, W. and T.Shibayama (1996) : Cross-shore Sediment Transport and Beach Deformation Model, Proc. 25th Int. Conf. on Coastal Eng., ASCE, pp.3062-3075.

Sato, S. and M.B.Kabiling (1994) : A Numerical Simulation of Beach Evolution Based on a Nonlinear Dispersive Wave-Current Model, Proc. 24th Int. Conf. on Coastal Eng., ASCE, pp.2557-2570.

Shimizu, T. (1995) : Derivation of an Experimental Method for Beach Change Considering Scale Effect and Applicability of the Method, Proc. Japanese Coastal Eng., Vol.42, JSCE, pp.621-625 (in Japanese).

Shimizu, T. (1988) : Similarity of Model Experiments on Onshore-offshore Beach Profile Change, CRIEPI Abiko Res. Lab. Rep. No.U87059 (in Japanese).

Shimizu, T. and M.Ikeno (1996) : Experimental Study on Sediment Transport in Surf and Swash Zones Using Large Wave Flume, Proc. 25th Int. Conf. on Coastal Eng., ASCE, pp.3076-3089.

Sleath, J.F.A. (1987) : Turbulent Oscillatory Flow over Rough Beds, J. of Fluid Mech., Vol.182, pp.369-409.

Sunamura, T. (1984) : Quantitative Predictions of Beach-Face Slopes, Geol. Soc. Am. Bull., Vol.95, pp.242-245.

Thornton, E.B. and R.T. Guza (1983) : Transformation of Wave Height Distribution, J. Geophys. Res., Vol.88, pp.5925-5938.